Dynamic spontaneous fluorescence in parametric wave coupling

Stefano Trillo
Fondazione Ugo Bordoni, Via B. Castiglione 59, 00142 Roma, Italy

Stefan Wabnitz
Laboratoire de Physique, Universite de Bourgogne, Avenue A. Savary, Boîte Postale 400, 21011 Dijon Cedex, France

(Received 13 November 1996)

Intense waves, subject to a parametric exchange of energy in dispersive media may spontaneously emit radiation at new frequencies. This effect represents a spatially dynamic version of parametric fluorescence with a single pump beam. Enhancement of the scattering into new frequencies is predicted near homoclinic or separatrix evolutions of the continuous-wave parametric processes. Examples of the decay of the coupled waves are given for three- and four-photon interactions. [S1063-651X(97)51105-6]

PACS number(s): 42.65.Yj, 03.40.Kf, 47.20.−k, 52.35.Mw

Spontaneous parametric fluorescence denotes the decay of an intense beam through the parametric (i.e., the total energy of the field is conserved, and the medium response is local and instantaneous) emission of sideband waves at frequencies $\omega\pm\Omega$ set by the energy selection rule $2\omega=(\omega+\Omega)+(\omega-\Omega)$ [1], or $\omega+\omega=(\omega+\Omega)+(\omega-\Omega)$ [2]. The maximum decay rate occurs for the wave-number matching or momentum conservation (i.e., $\mathbf{k}_{2\omega}=\mathbf{k}_{\Omega}+\mathbf{k}_{-\Omega}$ or $2\mathbf{k}_{\omega}=\mathbf{k}_{\Omega}+\mathbf{k}_{-\Omega}$, respectively), the bandwidth being generally determined by the dispersion. Whenever the wave-vector matching condition is tuned by the pump intensity, the parametric decay is also known as modulational instability (MI), which is widespread in physics [3–9]. MI is observed in fluids [5], optical dielectrics [6], plasmas [7,8], electrical circuits [9], and elastic waves [3]. Moreover, MI is closely related to the generation of solitons, which are the stable eigenmodes of the dispersive propagation. It represents the universal mechanism governing the transition from unstable plane waves into stable solitons in nearly conservative physical systems [4].

On the other hand, the parametric mixing of two or more intense waves is widespread in both quadratic or cubic nonlinear media. For instance, resonant wave interactions [10] constitute a flexible means to generate new frequencies, including the frequency degenerate wave coupling as a practically important case [11]. In analogy to a single wave, the propagation of multiple intense waves will also be subject to MI in dispersive or diffractive nonlinear media. Through the nonlinear susceptibility, the coupled waves introduce a periodic modulation of the dielectric constant. As a result, new frequencies are scattered off the initial beams. However, it appears that the MI of periodic parametric coupling has not been investigated yet. In fact, only the relatively simple case was considered when the waves do not exchange energy but simply induce a mutual nonlinear phase shift. For example, take two incoherently coupled waves in a cubic medium [12], or the nonlinear eigenmodes of second-harmonic generation (SHG) in a quadratic medium [13].

The purpose of this Rapid Communication is to show that coupled waves in nonlinear media are subject to the spontaneous scattering of energy into a spectrum of side modes. This effect provides *a fundamental limit to the effective interaction length of parametric interactions* [14]. As we shall see, the MI of periodically coupled waves *is particularly enhanced in the vicinity of homoclinic evolutions*, that are associated with saddle points in the phase space portrait describing the cw or homogeneous propagation.

Consider for example partially degenerate three-photon mixing or SHG. The total electric field reads $E(z,t)=E_1\exp(ik_1z-i\omega_0t)+E_2\exp(ik_2z-i2\omega_0t)$, and SHG is described by the coupled equations for the complex envelopes $u_1=\sqrt{2}E_1/\sqrt{P}$ and $u_2=E_2/\sqrt{P}$ $(P\equiv|E_1|^2+|E_2|^2)$ [8,13]

$$-i\frac{\partial u_1}{\partial\zeta}=\frac{\delta H^{(2)}}{\delta u_1^*}=-\frac{\beta_1}{2}\frac{\partial^2u_1}{\partial\tau^2}+u_2u_1^*\exp(i\kappa\zeta),$$

$$-i\frac{\partial u_2}{\partial\zeta}=\frac{\delta H^{(2)}}{\delta u_2^*}=-\frac{\beta_2}{2}\frac{\partial^2u_2}{\partial\tau^2}+\frac{u_1^2}{2}\exp(-i\kappa\zeta), \qquad (1)$$

where the field Hamiltonian $H^{(2)}=\int_{-\infty}^{+\infty}\mathcal{H}^{(2)}d\tau$ $[\mathcal{H}^{(2)}=u_1^2u_2^*\exp(i\kappa\zeta)/2+\text{c.c.}—\Sigma_{j=1,2}\beta_j|u_{j,\tau}|^2/2$ is the density], and the energy flux $Q=\int_{-\infty}^{+\infty}[|u_2|^2+|u_1|^2/2]d\tau$ are conserved along the propagation coordinate ζ. In Eqs. (1), the dimensionless units are $\zeta\equiv z/z_{nl}=z\epsilon_0\chi^{(2)}\sqrt{P}$, $\chi^{(2)}$ being the second-order susceptibility, the retarded time $\tau\equiv(t-z/v)/\sqrt{|k_1''|z_{nl}}$, with $\beta_j\equiv k_j''/|k_1''|$ $(k_j''=d^2k/d\omega^2|_{\omega=j\omega_0}$ are chromatic dispersions) and the wave-number mismatch $\kappa\equiv(k_2-2k_1)z_{nl}$.

A second example is four-photon mixing in a birefringent dielectric with cubic response [15]. The polarization changes of the field $\mathbf{E}=[\mathbf{x}E_x(z,t)\exp(ik_xz)+\mathbf{y}E_y(z,t)\exp(ik_yz)]\exp(-i\omega_0t)$ are represented by the coherently coupled nonlinear Schrödinger equations for the envelopes $u_{1,2}=E_{1,2}/\sqrt{P}$ of the two circular polarizations $E_{1,2}=(E_x\pm iE_y)\exp[i(k_x+k_y)z/2]$ [16],

$$-i\frac{\partial u_j}{\partial\zeta}=\frac{\delta H^{(3)}}{\delta u_j^*}=-\frac{\beta}{2}\frac{\partial^2u_j}{\partial\tau^2}+\frac{u_{3-j}}{2}+2p(|u_j|^2+\sigma|u_{3-j}|^2)u_j, \quad j=1 \text{ and } 2. \qquad (2)$$

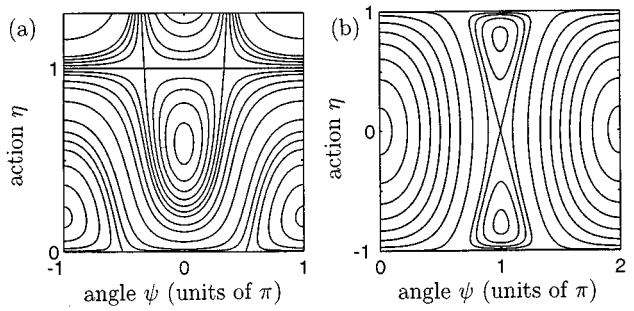

FIG. 1. Phase-space portraits of the stationary Hamiltonian in (a) quadratic ($\kappa=0.5$) or (b) cubic media ($p=0.8$).

Here $\zeta\equiv 2\pi z/z_b$, $z_b=2\pi/|k_y-k_x|$, and $\tau=(2\pi/|k_1''|z_b)^{-1/2}(t-z/v)$, $\beta=k''/|k''|$ (where $v^{-1}=dk_{x,y}/d\omega|_{\omega=\omega_0}$, and $k''=d^2k_{x,y}/d\omega^2|_{\omega=\omega_0}$), and p is a dimensionless power [e.g., for an optical fiber $p=4\pi n_2 P/(3A_{\rm eff}\lambda_0|k_y-k_x|)$, n_2 is the nonlinear index, $A_{\rm eff}$ is the effective area, and the cross-phase modulation coefficient $\sigma=2$ [16]]. The Hamiltonian density associated with Eqs. (2) $\mathcal{H}^{(3)}=-\Sigma_{j=1,2}\beta|u_{j,\tau}|^2/2+\frac{1}{2}(|u_1|^2+|u_2|^2)+p[|u_1|^4+|u_2|^4+\sigma|u_1|^2|u_2|^2]$, and the conserved photon flux is $Q=\int_{-\infty}^{+\infty}|u_1|^2+|u_2|^2 d\tau$. In Eqs. (1) and (2), we neglected, for the sake of simplicity, the group-velocity walk-off terms between the coupled waves; the present analysis can be easily extended to include those terms. Equations (1) and (2) also apply to describe MI due to wave coupling with diffraction in one dimension (τ representing a spatial transverse coordinate), which is the object of recent experiments [17].

The stationary dynamics (i.e., $\partial/\partial\tau=0$) of Eqs. (1) and (2) is integrable by quadratures. Explicit ζ-periodic solutions for $u_{1,2}\equiv\overline{u_{1,2}}(\zeta)$ are obtained in terms of the trajectories of the reduced equivalent one-dimensional anharmonic oscillator for the action-angle variables η,ψ,

$$\frac{d\eta}{d\zeta}=\frac{\partial H_r^{(m)}}{\partial\psi},\quad \frac{d\psi}{d\zeta}=-\frac{\partial H_r^{(m)}}{\partial\eta},\quad m=2 \text{ and } 3. \tag{3}$$

In SHG, $\overline{u_1}=\sqrt{2(1-\eta)}\exp(i\phi_1)$, $\overline{u_2}=\sqrt{\eta}\exp(i\phi_2-i\kappa\zeta)$, (where $|\overline{u_1}|^2/2+|\overline{u_2}|^2=1$), $\psi=\phi_2-2\phi_1$, and

$$H_r^{(2)}=H_r^{(2)}(\eta,\psi)=\kappa\eta+2\sqrt{\eta}(1-\eta)\cos\psi. \tag{4}$$

In the case of the vector nonlinear Schrödinger equations (2), we set $\overline{u_{1,2}}=\sqrt{(1\pm\eta)/2}\exp(i\phi_{1,2})$, and obtain

$$H_r^{(3)}=H_r^{(3)}(\eta,\psi)=-p\eta^2+\sqrt{1-\eta^2}\cos\psi, \tag{5}$$

where the action $\eta=|\overline{u_1}|^2-|\overline{u_2}|^2$ and the angle $\psi=\phi_1-\phi_2$. The phase portraits of the reduced systems (3)–(5) exhibit the spatially stable and unstable eigenmodes of the coupling process [15,18]. As shown by Fig. 1(a) for SHG, Eq. (4) yields that for $|\kappa|<2$ a separatrix (which is homoclinic to the saddle $[\eta=1,\psi=\pm\cos^{-1}(\kappa/2)]$) divides the phase plane into two domains of periodic orbits (the domain $\eta>1$ is not physically accessible). These domains are centered around two different phase-locked (i.e., with $\psi=0,\pi$) elliptic eigenmodes. In the case of Hamiltonian (5), the eigenmode with $\eta=0$ and $\psi=\pi$ is an unstable saddle for $p>0.5$. As shown by Fig. 1(b), a figure-of-eight separatrix splits the phase plane into three domains of periodic orbits about stable centers.

By definition, the spatially stable (centers) or unstable (saddles) eigenmodes of the cw dynamics do not lead to energy transfer between the waves. Instead, we are interested here in studying the MI's of parametrically coupled waves, that is, of the periodic solutions of Eqs. (3)–(5). This is done by inserting in Eqs. (1) and (2) the fields

$$u_j=[\sqrt{\eta_j(\zeta)}+a_j(\zeta,\tau)]\exp[i\overline{\phi_j}(\zeta)],\quad j=1 \text{ and } 2, \tag{6}$$

where $\eta_j=|\overline{u_j}|^2$, and the perturbing terms are taken of the form $a_j(\zeta,\tau)=\epsilon_{js}(\zeta)e^{i\Omega\tau}+\epsilon_{ja}(\zeta)e^{-i\Omega\tau}$. In SHG, we set $\phi_1=\phi_1$ and $\phi_2=\phi_2-\kappa\zeta$. From Eqs. (1), after linearizing in the perturbing terms, we obtain

$$-i\frac{\partial\epsilon_{1s}}{\partial\zeta}=[\overline{\Omega_1}-\sqrt{\eta}\cos\psi]\epsilon_{1s}+\sqrt{\eta}e^{i\psi}\epsilon_{1a}^*+\sqrt{2(1-\eta)}e^{i\psi}\epsilon_{2s}, \tag{7}$$

$$-i\frac{\partial\epsilon_{2s}}{\partial\zeta}=\left[\overline{\Omega_2}-\frac{1-\eta}{\sqrt{\eta}}\cos\psi\right]\epsilon_{2s}+\sqrt{2(1-\eta)}e^{-i\psi}\epsilon_{1s},$$

where $\overline{\Omega_j}\equiv\beta_j\Omega^2/2$. Equations (7) couple to the equations for $\epsilon_{1,2a}^*$, which may be simply obtained by conjugating Eqs. (7) under the exchange $s\leftrightarrow a$. A similar procedure can be applied to Eqs. (2) with $\phi_j=\phi_j$, and yields

$$-i\frac{\partial\epsilon_{1s}}{\partial\zeta}=\left[\overline{\Omega_1}+p(1+\eta)-\frac{\sqrt{1-\eta^2}}{2(1+\eta)}\cos\psi\right]\epsilon_{1s}+p(1+\eta)\epsilon_{1a}^*+p\sigma\sqrt{1-\eta^2}(\epsilon_{2a}^*+\epsilon_{2s})+\frac{e^{-i\psi}}{2}\epsilon_{2s}, \tag{8}$$

$$i\frac{\partial\epsilon_{1a}^*}{\partial\zeta}=\left[\overline{\Omega_1}+p(1+\eta)-\frac{\sqrt{1-\eta^2}}{2(1+\eta)}\cos\psi\right]\epsilon_{1a}^*+p(1+\eta)\epsilon_{1s}+p\sigma\sqrt{1-\eta^2}(\epsilon_{2a}^*+\epsilon_{2s})+\frac{e^{i\psi}}{2}\epsilon_{2a}^*.$$

The above equations are coupled to similar expressions for ϵ_{2s} and ϵ_{2a}^*, obtained from Eqs. (8) with $1\leftrightarrow 2$, $\eta\rightarrow-\eta$, and $\psi\rightarrow-\psi$.

The perturbation equations (7) and (8) are of the form $\dot{\boldsymbol{\epsilon}}=M(\zeta)\boldsymbol{\epsilon}$, where $\boldsymbol{\epsilon}=(\epsilon_{1s},\epsilon_{1a}^*,\epsilon_{2s},\epsilon_{2a}^*)^T$ (T denotes transposition), and $M=M(\zeta)$ is a periodic (with period, say, ζ_P) 4×4 coefficient matrix associated with a given trajectory of the cw coupling process. The stability analysis of periodic linear ordinary differential equations is well known, and is based on the evaluation of the critical exponents according to Floquet (or Bloch) theorem [3]. These exponents are obtained from the 4×4 principal solution matrix, say $S\equiv\{\boldsymbol{\epsilon}^{(j)}(\zeta_P),\ j=1,2,3,\text{ and }4\}$, which represents the evaluation at $\zeta=\zeta_P$ of the independent set of solutions $\boldsymbol{\epsilon}^{(j)}(\zeta_P)$ of the linear periodic system. These solutions correspond to the initial conditions $S(\zeta=0)=I=\text{diag}\{1\}$. The eigenvalues $\lambda\equiv\exp(\mu+i\rho)$ of S such that $|\lambda|>1$ lead to the amplifica-

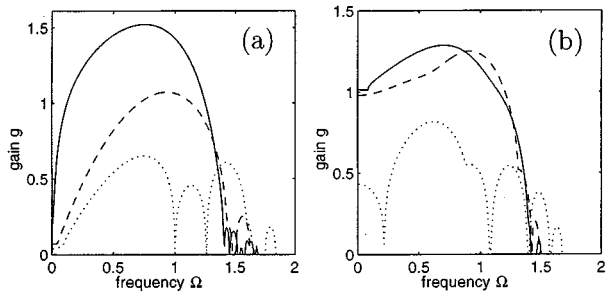

FIG. 2. MI gain g vs frequency Ω, for (a) a quadratic medium with $\kappa=0.5$ (dotted), 0.1 (dashed), 10^{-4} (solid), or (b) a cubic medium with $p=0.6$ (dotted), 0.95 (dashed), and 1.05 (solid).

tion of a small perturbation [3]. Hence the coupled cw's are unstable with respect to the growth of sidebands with the detuning Ω. The growth rate of the unstable sidebands is given by $g\equiv 2\ln|\lambda|/\zeta_P$. In the special case where the cw or homogeneous solutions are close to a stable eigenmode (elliptic point) of Eqs. (3)–(5), $|\lambda|\rightarrow\exp(\mu)$ and the critical exponent yields the MI gain $g=2\mu/\zeta_P$, ζ_P being the period for small oscillations about the fixed point.

We select as specific examples the stability of parametric mode coupling with initial conditions involving the excitation of the u_1 mode only. In the first case considered here, this input leads to the usual SHG from the fundamental [14], whereas the linear coupling leads to a periodic energy transfer between the two circular waves [15]. For the calculation of the critical exponents of the perturbation equations, the explicit solutions of Eqs. (3) should be entered in $M(\zeta)$. In the case of SHG, the first of Eqs. (3) yields $\eta(\zeta)=c_3+(c_2-c_3)\mathrm{sn}^2(g\zeta|k)$, where the period $\zeta_P=2K(k)/\sqrt{c_1-c_3}$, and $c_1>c_2>c_3$ are implicitly defined by the algebraic equation $(\eta-c_1)(\eta-c_2)(\eta-c_3)=\eta^3-(2+\kappa^2/4)\eta^2+(1+\kappa H_r)\eta-H_r^2/4, k^2=(c_2-c_3)/(c_1-c_3)$, $g=\sqrt{c_1-c_3}$. When the SH is generated without initial seeding, the above expression simplifies ($c_3=0$). The second of Eqs. (3) reads $\dot{\psi}=(\kappa/2)[1+c_2\mathrm{sn}^2(\sqrt{c_1}\zeta|k)]/[1-c_2\mathrm{sn}^2(\sqrt{c_1}\zeta|k)]$, which can be solved by means of the incomplete elliptic integral of the third kind in the so-called circular case [19]. Figure 2(a) shows the resulting instability growth rate $g=g(\Omega)$, for three different choices of κ. As can be seen, whenever the mismatch κ is chosen so that the trajectory in the (η,ψ) plane is in the vicinity of the separatrix (this is obtained for $\kappa=0$ with $\eta=0$), the MI gain is enhanced. Note also that the MI growth rate for scattering into side modes with a finite frequency shift Ω is always larger than the cw gain (for $\Omega=0$).

For polarization coupling (5), the initial u_1 mode is represented by $\eta(\zeta=0)=1$: this condition is homoclinic to the unstable saddle in Fig. 1(b) for $p=1$. Otherwise, the solution of Eqs. (5) involves either polarization rotations for $p<1$, or polarizations oscillations for $p>1$ [see Fig. 1(b)]. In the first case, Eqs. (3) and (5) yield $\eta=\mathrm{cn}(\zeta|k)$, and $\psi=\tan^{-1}[\mathrm{dn}(p\zeta|k)/(p\,\mathrm{sn}(\zeta|k))]$, with a period $\zeta_P=4K(k)$ and $k^2=p^2$, whereas, in the latter case $\eta=\mathrm{dn}(p\zeta|k)$, $\psi=\tan^{-1}[\mathrm{cn}(p\zeta|k)/\mathrm{sn}(\zeta|k)]$, and the period is $\zeta_P=2K(k)/p$, with $k^2=p^{-2}$. Note that $\zeta_P(p\rightarrow 1^+)\rightarrow 2\zeta_P(p\rightarrow 1^-)$. As shown by Fig. 2(b), again the side modes gain is enhanced for $p\rightarrow 1$, that is, whenever the separatrix is approached.

The predictions of the linear stability analysis are well confirmed by the full numerical solutions (by the so-called split-step method) of Eqs. (1) and (2), with the weakly perturbed initial conditions $u_{1,2}(\zeta=0,\tau)=\overline{u}_{1,2}(0)+\epsilon_{1,2}\cos(\Omega\tau)$. We set the initial sideband seed $\epsilon_{1,2}=10^{-4}$ to reduce the length scale for the development of the MI. Similar results are obtained with a broadband white noise seed. Figure 3 corresponds to SHG [$\overline{u_1}(0)=\sqrt{2}$, $\overline{u_2}(0)=0$] close to phase matching ($\kappa=10^{-4}$). Figure 3(a) shows the intensity evolution is fundamental over three periods ($\zeta=3\zeta_P$),

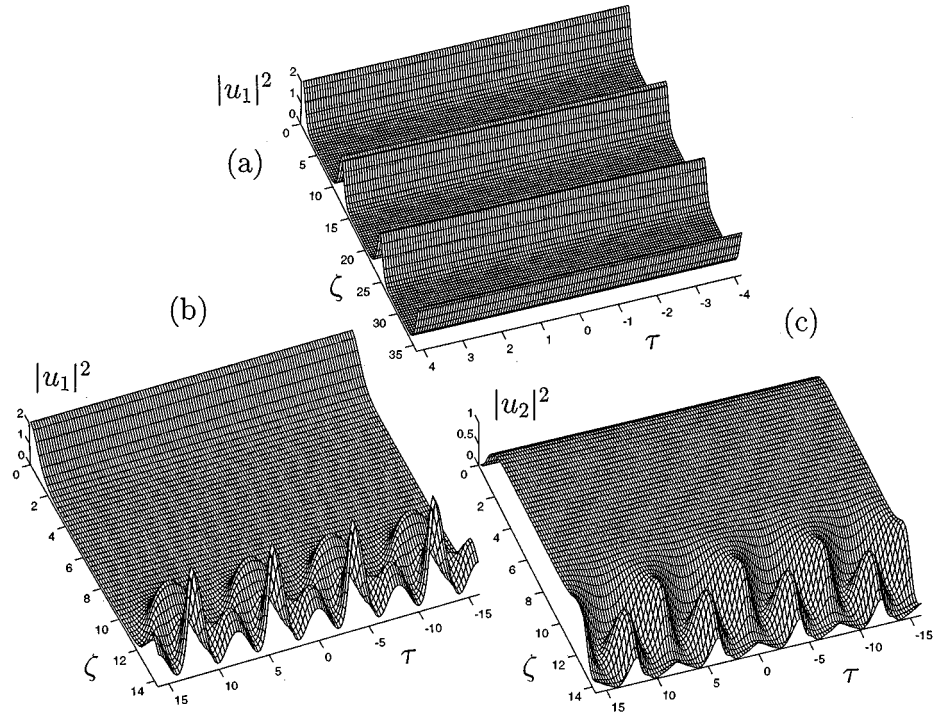

FIG. 3. Field evolution in SHG with $\eta(0)=0$, $\kappa=10^{-4}$, and normal dispersion ($\beta_{1,2}=1$): (a) intensity $|u_1|^2$ for $\Omega=3$, outside the MI gain bandwidth. (b) Same as (a) for the peak gain detuning $\Omega\simeq 1$. (c) Same as (b) for $|u_2|^2$.

when the seed frequency detuning is chosen outside the linear MI gain bandwidth (i.e., $\Omega=3$). As can be seen, the spatial evolution of the fundamental remains close to the unperturbed near-separatrix trajectory of the cw picture. Conversely, Figs. 3(b)–3(c) show that, whenever the perturbation frequency is close to the peak spectral gain (i.e., for $\Omega\simeq 1$), the growth of the side mode (and its harmonics) leads to the complete decay from the cw trajectory. This occurs even before that any back-conversion of the second harmonic wave into the fundamental (at the end of the first period of the cw evolution) has ever taken place. For longer interaction distances, a cascade of higher-order sideband pairs is observed. One may then conclude that the maximum length for observing periodic energy conversion in dispersive quadratic media (in particular close to phase matching, i.e., for $\kappa\simeq 0$), *is fundamentally limited by the parametric scattering introduced by* MI.

A similar statement also applies to four-photon processes. Figure 4 shows the spatial evolution of power in the right-circular u_2 mode, as it is obtained from the numerical solution of Eqs. (2) with $\overline{u_1}(0)=1$, $\overline{u_2}(0)=0$ ($\beta=1$, $\sigma=2$). In Fig. 4(a) [4(b)], p is slightly below (above) the critical value $p=1$ that leads to a homoclinic trajectory for the polarization state. As can be seen, the initial stage of the evolution of the circular polarization component is either a complete rotation [see Fig. 4(a) with $p=0.95$, which gives the polarization coupling period $\zeta_P=10.4$] or a libration with halved period [Fig. 4(b), $p=1.05$, $\zeta_P=4.9$]. The period doubling is associated with the crossing of the separatrix trajectory at $p=1$ [see Fig. 1(b)]. However, Fig. 4 clearly shows that the build-up of unstable side modes draws a substantial amount of energy from both polarization components of the field, which results in the effective depolarization of the intense beam in long-range evolutions.

In summary, we have shown that MI provides a general

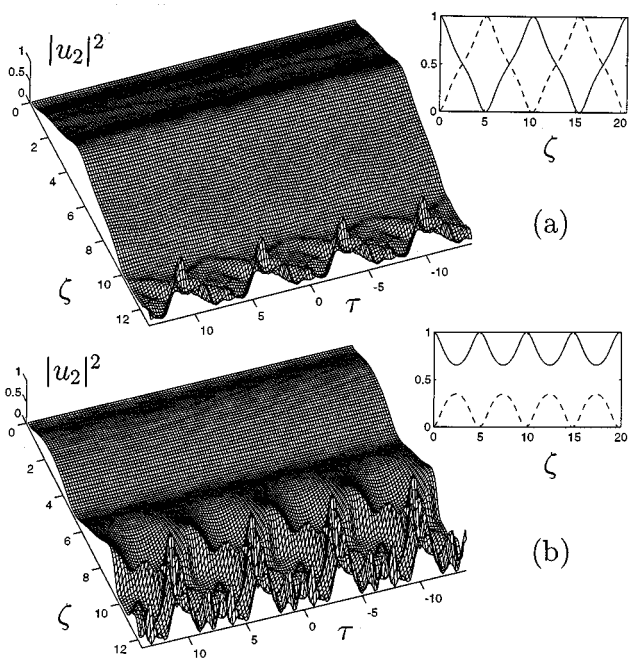

FIG. 4. Evolution of left-circular intensity $|u_2|^2$ with right-handed input and a seed with $\Omega=0.9$: (a) rotation for $p=0.95$ and $\zeta=1.25\zeta_P$; (b) oscillation for $p=1.05$ and $\zeta=2.5\zeta_P$. Insets show cw $|u_1|^2$ (solid) and $|u_2|^2$ (dashed) evolutions.

mechanism of instability for parametrically coupled waves, that periodically exchange energy in conservative dispersive nonlinear media. Our results are valid for a generic resonant wave coupling (including the degenerate cases), and can be applied to a variety of physical systems. These instabilities are particularly enhanced for any initial condition in the vicinity of the separatrices associated with the cw or homogeneous dynamics.

[1] S. E. Harris, M. K. Oshman, and R. L. Byer, Phys. Rev. Lett. **18**, 732 (1967).
[2] R. Y. Chiao, P. L. Kelley, and E. Garmire, Phys. Rev. Lett. **17**, 1158 (1966).
[3] A. H. Nayfeh and D. T. Mook, *Nonlinear Oscillations* (Wiley, New York, 1979), pp. 273–283 and 583–590.
[4] E. Infeld and G. Rowlands, *Nonlinear Waves, Solitons, and Chaos* (Cambridge University, Cambridge, 1990).
[5] G. B. Whitham, J. Fluid Mech. **22**, 273 (1965); T. B. Benjamin and J. E. Feir, *ibid.* **27**, 417 (1967).
[6] V. I. Bespalov and V. I. Talanov, Pis'ma Zh. Eksp. Teor. Fiz. **3**, 471 (1966) [JETP Lett. **3**, 307 (1966)]; K. Tai, A. Hasegawa, and A. Tomita, Phys. Rev. Lett. **56**, 135 (1986).
[7] T. Taniuti and H. Washimi, Phys. Rev. Lett. **21**, 209 (1968).
[8] V. E. Zakharov, S. L. Musher, and A. M. Rubenchik, Phys. Rep. **129**, 285 (1985); A. A. Kanashov and A. M. Rubenchik, Physica D **4**, 122 (1981).
[9] J. M. Bilbault *et al.*, Phys. Rev. E **51**, 817 (1995).
[10] G. M. Nedlin *et al.*, Phys. Rev. Lett. **77**, 3267 (1996).
[11] A. Yariv, *Quantum Electronics* (Wiley, New York, 1989).
[12] A. L. Berkhoer and V. E. Zakharov, Zh. Eksp. Teor. Fiz. **58**, 903 (1970) [Sov. Phys. JETP **31**, 486 (1970)]; G. P. Agrawal, Phys. Rev. Lett. **59**, 880 (1987).
[13] S. Trillo and P. Ferro, Opt. Lett. **20**, 438 (1995); Phys. Rev. E **51**, 4994 (1995); A. V. Buryak and Yu. S. Kivshar, Opt. Lett. **19**, 1612 (1994); Phys. Rev. A **51**, R41 (1995).
[14] J. A. Armstrong *et al.*, Phys. Rev. **6**, 1918 (1962).
[15] K. Sala, Phys. Rev. A **29**, 1944 (1984); G. Gregori and S. Wabnitz, Phys. Rev. Lett. **56**, 600 (1986); S. Trillo *et al.*, Appl. Phys. Lett. **49**, 1224 (1986).
[16] S. Wabnitz, Phys. Rev. A **38**, 2018 (1988); G. Cappellini and S. Trillo, *ibid.* **44**, 7509 (1991); S. Trillo and S. Wabnitz, Phys. Lett. A **159**, 252 (1991); S. G. Murdoch *et al.*, Opt. Lett. **20**, 866 (1995).
[17] R. A. Fuerst, D. M. Baboiu, B. Lawrence, W. E. Torruellas, G. I. Stegeman, S. Trillo, and S. Wabnitz, Phys. Rev. Lett. **78**, 2756 (1997).
[18] S. Trillo *et al.*, Opt. Lett. **17**, 637 (1992).
[19] P. Byrd and M. Friedman, *Handbook of Elliptic Integrals for Engineers and Physicists* (Springer, Berlin, 1971).